CHEMICAL CONSTITUENT DISTRIBUTION WITHIN MULTILAYERED CELL WALLS OF MOSO BAMBOO FIBER TESTED BY CONFOCAL RAMAN MICROSCOPY

Penglian Wei
Graduate Student
E-mail: ztzxwpl@163.com

Jianfeng Ma
Graduate Student
E-mail: Majf@icbr.ac.cn

Zehui Jiang
Professor
E-mail: Jiangzehui@icbr.ac.cn

Rong Liu
Graduate Student
E-mail: rowan_lr@163.com

Xin An
Graduate Student
E-mail: anxin@icbr.ac.cn

*Benhua Fei**
Professor
International Center for Bamboo and Rattan
Beijing, China
E-mail: feibenhua@icbr.ac.cn

(Received June 2015)

Abstract. Distribution of cellulose and lignin is key to physical and mechanical properties of woody materials. This study was carried out to investigate chemical constituent distribution of Moso bamboo (*Phyllostachys pubescens*) fiber using confocal Raman microscopy (CRM) with a particular focus on its unique multilayered structure. The results showed that syringyl and guaiacyl units of lignin were widely distributed across the whole cell wall, including the cell corner (CC) and compound middle lamella (CML), whereas p-hydroxyphenyl units were mainly located in the CC and CML regions. A series of CRM images of bamboo fiber cell walls confirmed that different concentrations of specific chemicals were present in the multilayered structure. Lignin concentration did not always decline from the periphery to the central part but sometimes increased close to lumen edges as well as some layers. Furthermore, variation of lignin and cellulose concentration across the cell wall could be obtained by using the line scanning function. Distribution difference of lignin and cellulose was generally located in the CML and lumen side as well as some borders between two adjacent secondary layers. The results from this study will deepen the understanding of the organization of Moso bamboo cell walls.

Keywords: *Phyllostachys pubescens*, confocal Raman microscopy, Raman imaging, chemical constituent distribution, cell wall.

* Corresponding author

INTRODUCTION

Bamboo, an important biomass resource around the world, has unique cell wall structure and excellent material properties. In addition to the special morphology structure of bamboo stems, the multilayered cell wall structure of bamboo fibers exhibits alternating broad and narrow lamellae (Parameswaran and Liese 1976; Lybeer and Koch 2005a; Lybeer et al 2006; Mustafa et al 2011). This alternating hierarchical structure is distinguished from the typical three-layered secondary wall of wood and is considered to be one of the factors that contribute to the high tensile strength of bamboo (Gritsch et al 2004).

Plant cell walls are mainly composed of cellulose, lignin, and hemicellulose. It is well known that cellulose, lignin, and hemicellulose have different contributions to cell wall properties. Komuraiah et al (2014) investigated Pearson rank correlation coefficients between composition and properties of several natural fibers. They found that tensile strength and Young's modulus of plant fibers increased with cellulose content but decreased with hemicellulose content. Zhang et al (2013) investigated the effects of lignin and hemicellulose content on mechanical properties of single Chinese fir tracheids using single-racheid-test technology in an environment of 23°C and 25% RH. They confirmed that tensile strength of single tracheids increased with lignin degradation, whereas it decreased with hemicellulose degradation. The previous studies confirmed that cell wall properties were deeply affected by the amounts and intrinsic characteristics of cell wall components. Thus, it is essential to know how chemical constituents are distributed in multilayered cell walls. It is helpful to deeply understand the mechanical properties and ingenious design of bamboo fiber cell walls.

Several techniques such as transmission electron microscopy (He et al 2002; Lybeer and Koch 2005a; Wi et al 2014), scanning electron microscope/energy dispersive using X-ray analysis (Saka and Thomas 1982; Ma et al 2011), and ultraviolet (UV) or visible microscopy (Lin et al 2002; Lybeer and Koch 2005b), and fluorescence microscopy (Donaldson et al 2001) were used to investigate chemical constituent distribution of biomass materials. The disadvantages of these methods include complex sample preparation processes (such as embedding, staining, or antibodies tagged) and strong specificity that cannot obtain information of multiple components at the same time. Raman spectroscopy is an efficient vibrational spectroscopic tool in the investigations of chemical components of plant materials (Larsen and Barsberg 2010). It can study both lignin and cellulose simultaneously in a noninvasive way and provide chemical information in situ with high spatial resolution (Gierlinger and Schwanninger 2007; Richter et al 2011). Samples used for Raman testing do not need any further prepared processes such as staining, embedding, dehydration, isolation, or other chemical pretreatment. Furthermore, Raman microscopy is less sensitive to water, which made the sample preparation and testing process easy to carry out (Gierlinger et al 2012). Thus, Raman spectroscopy analysis is a fast procedure and very suitable for studies of hydrated biological materials.

Raman spectroscopy was successfully used to investigate wood and nonwood plant cell walls. Röder et al (2004) studied the topochemical distribution of lignin in individual cell wall layers of beech wood. They found that confocal Raman spectroscopy and UV micro spectrophotometry could be valuable complementary techniques to study distribution of lignin and cellulose on a subcellular level. Richter et al (2011) used a Raman imaging approach to reveal the functional plant cell wall design of *Phormium tenax* leaf. They successfully obtained pectin and lignin distribution within different tissue at different positions and predicted microfibril angle based on selective extracted spectra from Raman images. Merk et al (2014) successfully gained the spatial distribution of colloidal iron oxide in hybrid wood materials with magnetic anisotropy by Raman spectroscopic mapping. These applications confirmed the power of Raman microscopy in chemical constituent distribution research, but few applications have been found in bamboo cell walls, based on the literature. Wang et al (2012, 2014)

investigated lignin distribution and cellulose orientation of bamboo fibers with Raman spectroscopy. They found that cell corners (CCs) and compound middle lamella (CML) were heavily lignified compared with secondary cell walls. Cellulose content was greater in secondary cell walls than in CCs and CML. However, the details of chemical constituent distribution within a single cell wall are not fully understood. The objective of this study was to investigate the characteristics of chemical constituent distribution in situ in bamboo fiber cell walls using confocal Raman microscopy and to focus on lignin and cellulose variation within different cell wall lamella.

MATERIALS AND METHODS

A 6-yr-old Moso bamboo *Phyllostachys pubescens* culm, total height of 15.5 m and diameter at breast height of 11.3 cm, was harvested from a plantation in Huangshan, Anhui Province, China. Blocks about 20-30 mm long were cut along the grain from the middle part of the 10th internode (numbered from the ground level) and stored in a refrigerator to keep fresh. Without any further preparation, 10-μm-thick transverse sections located at about the middle part of the culm wall were cut from the freshly kept blocks on a sliding microtome (SM2000R, Leica Microsystems, Wetzlar, Germany) equipped with a tungsten steel knife and were immediately placed on a glass slide. A drop of distilled water was added, and a cover slip was placed on top of the samples. To avoid evaporation of water during the subsequent Raman test, nail polish was used to seal around the cover slip.

Raman spectra were acquired with an Renishaw InVia confocal Raman microscope (Wotton-under-Edge, Gloucestershire, UK) equipped with a motorized xyz stage. To achieve great spatial resolution, measurements were conducted with a high numerical aperture (NA) microscope objective (100×, oil, NA = 1.40, Leica) and a linearly polarized green laser (λ = 532 nm) was used for excitation. Raman light was detected by an air-cooled, back-illuminated spectroscopic charge-coupled device camera behind a grating (1800 g/mm) spectrograph with a spectral resolution of 2 cm^{-1}. Wire 4.1 software (Renishaw) was used for measurement setup and controlled the microscope as well as image processing. For imaging, the fast scanning function with an exclusive StreamLine HR mode was used to significantly increase mapping speed. To achieve high spatial resolution imaging, spectra acquirements were done at every 0.3-μm step size with an integration time of 0.66 s. Different chemical images were generated by using a sum filter, integrating across defined bands of the spectrum. For spectroscopic analysis, extended integration times (10 s) were used to increase signal-to-noise ratio and acquire spectra with sufficient detail. For single or double cell wall line scanning, 0.1-μm step size and 3-s integration time were used for measurement setup to get more information about the chemical constituent distribution within each cell wall layer.

RESULTS AND DISCUSSION

Multilayered Structure of Bamboo Fiber Cell Wall

Bamboo fibers exhibit typical multilayered cell wall structure. These multilayered fibers aggregate together to form a fiber cap and compose a vascular bundle that shows inhomogeneous distribution across the culm wall, such as dense dispersal in the outer part and sparse dispersal in the inner part (Fig 1a). A bright field image of one fiber cap located in the middle zone of a bamboo culm wall is shown in Fig 1b. The observed fibers had different degrees of layered structure based on their localization within the fiber cap. Fibers with greatly layered structure were mainly distributed in the periphery of the fiber cap. These fibers consisted of several discernible sublayers (Fig 1c). Most fibers in the inner part of the fiber cap had fewer layers than did periphery fibers (Fig 1d). Gritsch et al (2004) established a classification system to investigate distribution of fibers with different amounts of layers in fiber caps. In the classification system, cell wall layers included two types, namely a thin

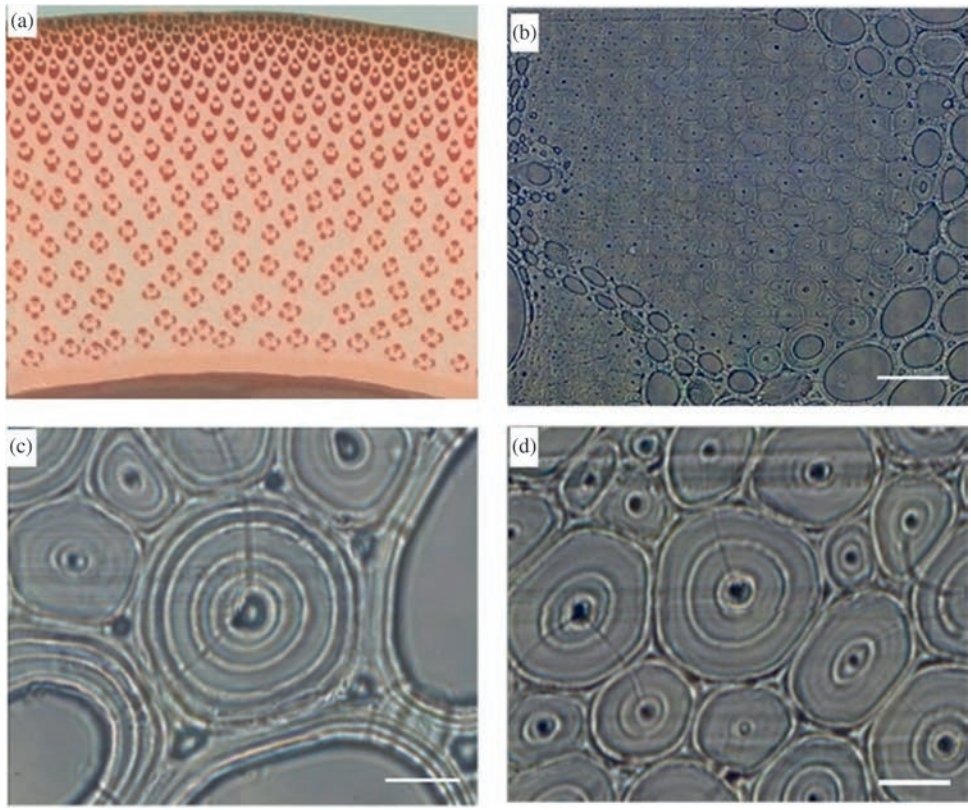

Figure 1. The anatomical structure of a bamboo culm wall and bamboo fiber. (a) Culm wall of Moso bamboo. Vascular bundles were unevenly distributed across the culm wall. (b) One fiber cap located in middle zone of a culm wall. Large and significant layered fibers were mainly distributed in peripheral regions of fiber cap. (c) Typical highly layered bamboo fiber cell. (d) Morphology of majority bamboo fiber cells. Scale bar: (b) 50 μm, (c and d) 10 μm.

layer and a broad layer. The thickness of thin layers was less than 300 nm (Parameswaran and Liese 1976), which cannot be observed under an optical microscope. Therefore, in this study, the cell wall layers only referred to those broad layers that could be observed directly with a distinct border.

Characteristic Raman Spectrum

Most polymers in plant cell walls have a Raman fingerprint based on vibrational modes of their substructural units or groups. The characteristic Raman spectra collected from different cell wall regions of bamboo fibers, namely CC, CML, inner secondary cell (ISC) wall layer, and outer secondary cell (OSC) wall layer, are shown in Fig 2. In all spectra, a high fluorescence background (causing a shift in the Raman intensity axis) was observed, which was caused by high lignin content reflected by the high lignin peak around 1598 cm^{-1} (Agarwal and Ralph 1997; Gierlinger and Schwanninger 2007; Sun et al 2010). This was somewhat different from a wood cell wall with high fluoresce background, primarily originating from the CC region (Gierlinger and Burgert 2006), indicating that bamboo had a greater lignification level in the secondary cell wall.

Pronounced differences were found in two major band regions in the spectra. One region was 1000-1300 cm^{-1} in which significant difference arose at three band positions, ie 1094, 1172, and 1204 cm^{-1}. The peak of 1094 cm^{-1}, a cellulose-orientation-sensitive band (Edwards et al 1997;

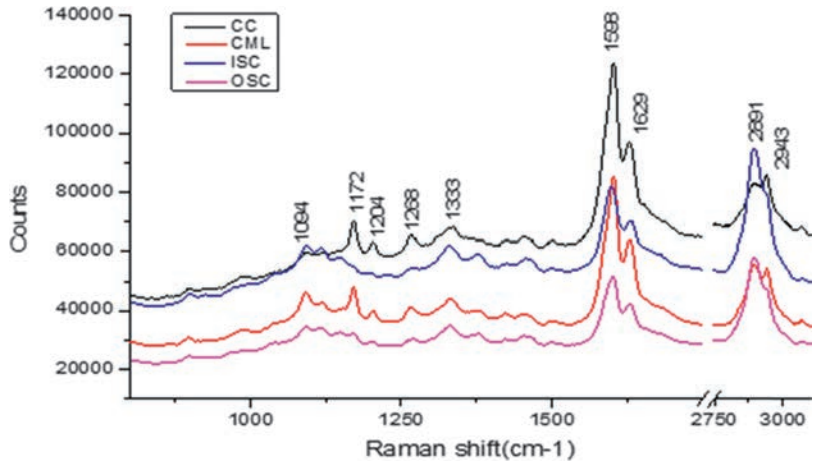

Figure 2. Raman spectrum of different cell wall regions; bands at 1024, 1268, 1333, and 1598 cm^{-1} were caused by lignin, and 1172 and 1629 cm^{-1} were caused by hydroxycinnamic acids. Cellulose contributions were present at 1094 and 2891 cm^{-1}. Band at 2943 cm^{-1} was caused by methoxy groups (Agarwal and Ralph 1997; Ram et al 2003; Saariaho et al 2003; Sun et al 2012). CC, cell corner; CML, compound middle lamella; OSC, outer secondary cell wall layer; ISC, inner secondary cell wall layer. All spectra were collected at 10-s exposure time.

Gierlinger et al 2012), was more significant in ISC and CML spectrum than in CC and OSC spectrum, reflecting different cellulose-chain-oriented directions in these regions. The peaks of 1172 and 1204 cm^{-1} were assigned to hydroxycinnamic acid and p-hydroxyphenyl unit of lignin, respectively (Ram et al 2003; Saariaho et al 2003; Sun et al 2010, 2012). The CC and CML spectrum differed clearly from ISC and OSC spectra because of additional bands at 1172 and 1204 cm^{-1}. This difference combined with the observation of another hydroxycinnamic acid peak at 1629 cm^{-1} (Ram et al 2003), which manifested in all spectra, indicated that H units and some kinds of hydroxycinnamic acid were mainly distributed in the CC and CML regions. Another key difference was found in the 2800-3000 cm^{-1} band region in which an obvious double peak in CC and CML spectrum turned into an intense peak with another peak as a shoulder.

In the 1250-1700 cm^{-1} band region, the four spectrum was similar in shape but with different signal intensity in special peaks. All spectra showed characteristic peaks of guaiacyl and syringyl units of lignin at 1268 and 1333 cm^{-1}, respectively (Saariaho et al 2003; Sun et al 2010, 2012). This confirmed the wide distribution of G and S units in the cell wall, including CC and CML regions.

Chemical Constituent Distribution

Chemical images were generated by integrating across intensity of defined bands shown in the characteristic Raman spectra (Fig 2). Results of chemical images showed that signal distribution mainly comes from two macromolecules, lignin and cellulose. Basic morphology of measured cell walls became apparent in chemical images based on specific substance distribution (Fig 3). By integrating across the bands around 1598 cm^{-1} based on aryl ring stretching (Agarwal and Ralph 1997), spatial distribution of lignin was visualized (Fig 3a, c). Spectroscopic images showed that lignin concentrations were greatest in the CC and CML regions and gradually decreased into the secondary cell wall. Interestingly, the lignin concentration did not always decrease in the secondary cell wall but increased in some layers. In situations of less layered fiber cells (Fig 3a), the outer broad layer (corresponding to L3 in Fig 3b) showed lighter signal intensity compared with the inner broad layer (corresponding to L4 in Fig 3b) and surrounding

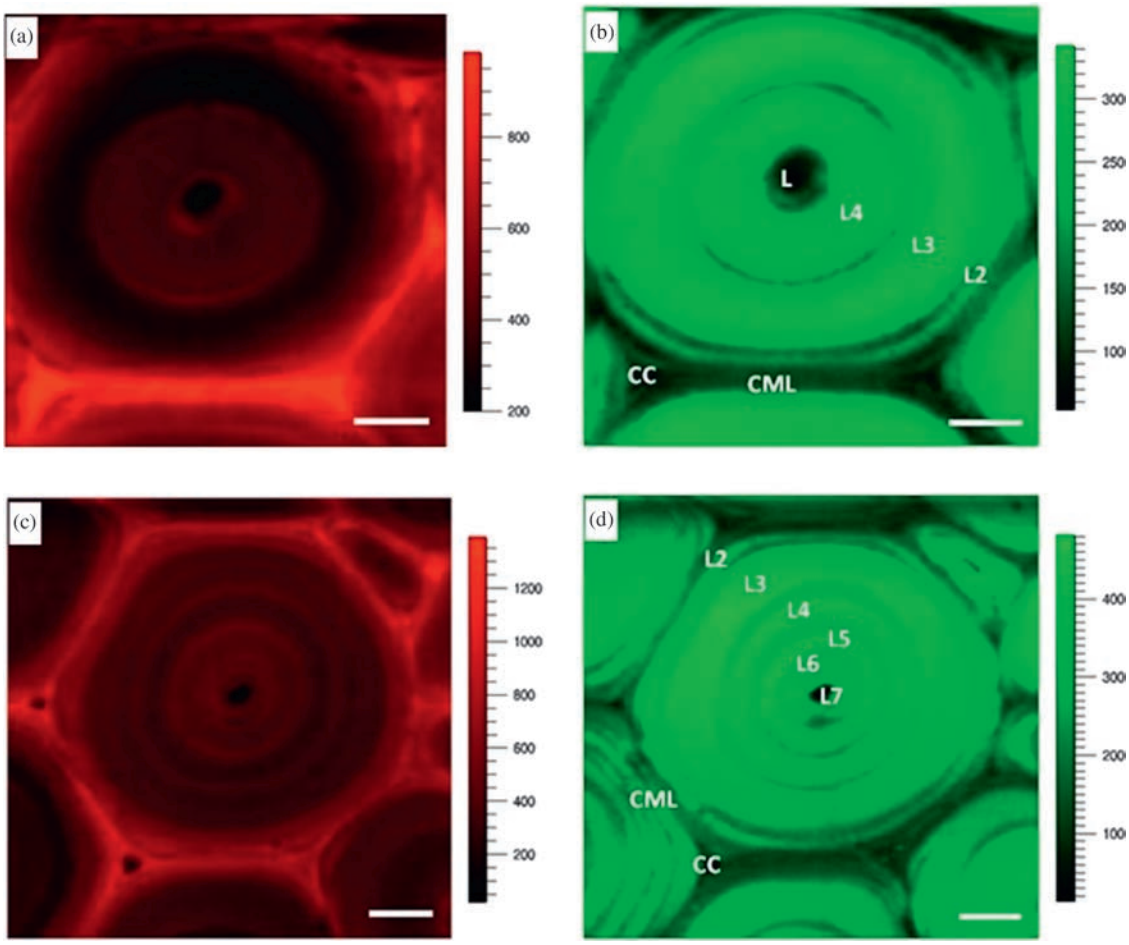

Figure 3. Raman spectroscopic images show distribution of lignin and cellulose in a single bamboo fiber. (a) Lignin distribution in a four-layered bamboo fiber cell. Bright red areas indicate high concentration of lignin, and dark red areas correspond to low lignin concentration. (b) Distribution of cellulose in the same fiber cell shown in Fig 3a. Bright and dark green areas correspond to high and low concentration of cellulose, respectively. (c) Lignin distribution in bamboo fiber cell with seven layers. (d) Cellulose distribution of the same fiber cell shown in Fig 3c. CC, cell corner; CML, compound middle lamella; L, lumen; L2, L3, L4 . . . represent different cell wall layers successively from periphery to lumen direction for each single fiber cell, respectively. Scale bar: 5 μm.

CML. This indicated a lower lignin concentration in the outer broad layer. In highly layered fiber cells (Fig 3c), three lignin-concentrated layers (L5, L6, and L7 in Fig 3d) with brighter color compared with other outer layers (L3 and L4 in Fig 3d) were found around the lumen area. The lignin-concentrated layers had almost uniform lignin distribution in each individual layer and formed an outside core for lumens.

Parameswaran and Liese (1976) showed that thick-walled bamboo fibers had a polylamellate structure with alternating broad and narrow lamellae, and the concentration of lignin was higher in the narrow lamellae. In their definition, the narrow lamellae were extremely thin (∼300 nm), which is beyond the resolving power of Raman microscopy. In this study, obscure thin circular rings with greater Raman signal contrast appeared at each edge of adjacent

layers, which could indicate existence of lignin-dense narrow layers (Fig 3a, c). But lignin concentration in thin regions was significantly lower than that of CC and CML regions. This observation was somewhat different from the results reported by Parameswaran and Liese (1976). They found that narrow lamella zones had similar lignin concentration to that of CML.

With integrating across the strong band at 2891 cm^{-1}, which was dominated by C-H stretching of cellulose (Gierlinger and Burgert 2006), cellulose-rich regions were emphasized (Fig 3b, d). Morphology of cell walls was even more obvious based on the cellulose distribution. The relatively narrow layer (L2 in Fig 3b, d) beside the outermost broad layer, which cannot be observed in the corresponding lignin distribution image (Fig 3a, c), was appearing. The lowest cellulose concentration was found in the CC and lumen regions, followed by border regions between two neighboring layers. Except for differences at CC, lumen regions, and border regions between two neighboring layers, cellulose concentration was uniform within other regions.

With comparison of lignin and cellulose distribution across whole cell walls (Fig 3), a reverse distribution relationship of lignin and cellulose can be found in CC, CML, and borders between different layers. These regions had relatively greater lignin concentration and lower cellulose concentration. Within various secondary layers, there was no obvious relationship between lignin and cellulose distribution.

From the analysis of relationships between strength and gradient structures of bamboo (Amada et al 1997), it was found that bamboo is an optimized natural composite that can be regarded as a functionally graded material. The concept of functionally graded materials could be considered as gradual substance distribution. The inhomogeneous distribution of vascular bundles across bamboo culm walls, ie dense dispersal in the outer part and sparse dispersal in the inner part, can be regarded as a macroscopic gradual distribution. Although at cell level, gradual substance distribution still exists, ie uneven distribution of lignin, which has been observed to be highly concentrated in CC and CML regions and tends to gradually decrease in the secondary cell wall.

Line Scanning

To get detailed insights into variability and distribution of lignin and cellulose concentration in various parts of a fiber cell wall, a line scanning technique was used to generate line profiles on transverse sections (Fig 4a, c). Line profiles were acquired by monitoring variation of lignin (at 1598 cm^{-1}) and cellulose (at 2891 cm^{-1}) Raman band intensity, with a step size of 100 nm (Fig 4b, d). Positions of each cell wall layer could be matched accurately with an intensity curve based on the position-resolved function of the motorized xyz stage. As expected, cellulose concentration was invariable in most secondary cell wall layers, except for regions near to the lumen and CML in which a significant decrease in cellulose content could be observed (Fig 4b, d). This distribution pattern corresponded to the Raman imaging results (Fig 3b, d). Lignin concentration was more variable across a single cell wall, especially in highly layered fiber. In the case of less layered fiber (Fig 4a), as the scan moved from the left lumen side to the right CML region, lignin concentration increased to a relatively higher value at the edge of the lumen, then gradually decreased, stayed steady, and finally increased close to the CML. In the case of highly layered fiber (Fig 4c), the change in lignin concentration in layer L6 and L7 was not significant. As the scan moved from left to right, it detected a drop in lignin concentration in layer L5, a gradual rise in layer L4, another drop in layer L3, a significant rise in layer L2, and a dramatic rise after a sudden drop in the CML. To compare relative distribution of lignin and cellulose, lignin Raman signal intensity along the segment points was divided by cellulose Raman signal intensity. As shown in Fig 4b, d, the impact of high lignin and low cellulose concentrations of CML and its adjacent layer was obvious. The lumen interface and some borders between two adjacent secondary layers also had a greater lignin-to-cellulose ratio compared with most secondary layers. This indicated that

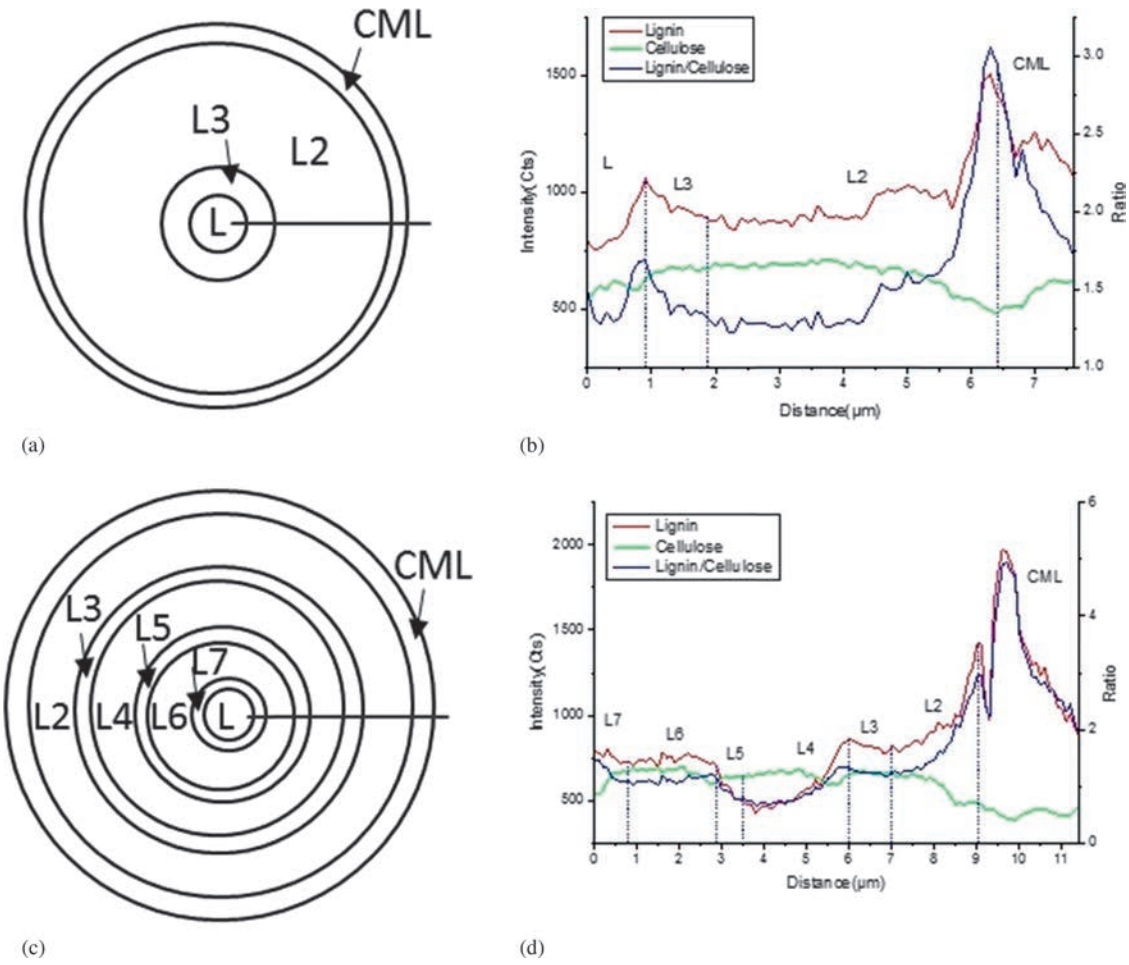

Figure 4. Line scanning showing lignin and cellulose concentration variation across bamboo fiber cell walls. (a) Morphology of the tested bamboo fiber with three layers. The scanning path is shown by the black solid line. (b) Intensity curve shows lignin and cellulose concentration variation along the scanning path corresponding to Fig 4a. (c) Morphology of the tested bamboo fiber with a highly layered structure. Line scanning path is represented by the black solid line. (d) Intensity curve along the scanning path corresponding to Fig 4c; Different cell wall layers are named sequentially as CML, L2, L3 . . . from the periphery toward the lumen for each single fiber cell. CML, compound middle lamella; L, lumen; L2, layer two; L3, layer three; L4, layer four; L5, layer five; L6, layer six; L7, layer seven.

the CML, lumen edge, and interface between two adjacent layers were relatively enriched in lignin.

The trend of increasing lignin concentration from the lumen side to the CML was found in single fiber cell walls. This indicated that lignin could first deposit in peripheral regions of a cell and then proceed toward the lumen side. However, the trend of gradual decrease from one side to another side was not found in all single layers. There were some layers in which the lignin concentration was almost invariable, eg layer L6 in Fig 4c. There were also some layers with relatively low lignin concentration compared with other neighboring layers, eg layer L4 and L5 in Fig 4c. This phenomenon possibly indicated that bamboo has a complex regulatory mechanism for adjusting lignification of cell walls to fulfill multiple functions during cell wall formation.

CONCLUSIONS

In this study, Raman microscopy was used to generate images of lignin and cellulose distribution in multilayered cell walls of bamboo fiber with a high lateral resolution. Raman images indicated that concentration of lignin and cellulose varied, both within and between distinct sublayers. Cellulose had a relatively even distribution, whereas lignin concentration varied greatly within distinct cell wall layers, especially in highly layered fibers. Diversity of lignin distribution within highly layered cell walls indicated that macromolecular organization in the multilayered structure of bamboo fiber is very complex. Furthermore, avenues of research in the future could include investigation of differently distributed patterns of chemical constituents across different types and locations of cell walls to better understand the organization of bamboo cell walls.

ACKNOWLEDGMENTS

We acknowledge financial support by the National Natural Science Foundation of China (31370563). We also thank application engineer Wang Zhifang and assistant service manager Raman Liu Zhen at the Beijing Branch Office of Renishaw (Shanghai) Trading Co. Ltd for their help with Raman testing.

REFERENCES

Agarwal UP, Ralph SA (1997) FT-Raman spectroscopy of wood: Identifying contributions of lignin and carbohydrate polymers in the spectrum of black spruce (*Piceamariana*). Appl Spectrosc 51:1648-1655.

Amada S, Ichikawa Y, Munekata T, Nagase Y, Shimizu H (1997) Fiber texture and mechanical graded structure of bamboo. Compos, Part B Eng 28B:13-20.

Donaldson L, Hague J, Snell R (2001) Lignin distribution in coppice poplar, linseed and wheat straw. Holzforschung 55:379-385.

Edwards HGM, Farwell DW, Webster D (1997) FT Raman microscopy of untreated natural plant fibres. Spectrochim Acta 53:2383-2392.

Gierlinger N, Burgert I (2006) Secondary cell wall polymers studied by confocal Raman microscopy: Spatial distribution, orientation, and molecular deformation. N Z J For Sci 1:60-71.

Gierlinger N, Keplinger T, Harrington M (2012) Imaging of plant cell walls by confocal Raman microscopy. Nat Protoc 7:1694-1708.

Gierlinger N, Schwanninger M (2007) The potential of Raman microscopy and Raman imaging in plant research. Spectroscopy 21:69-89.

Gritsch CS, Kleist G, Murphy RJ (2004) Developmental changes in cell wall structure of phloem fibres of the bamboo *Dendrocalamusasper*. Ann Bot 94:497-505.

He XQ, Suzuki K, Kitamura S, Lin JX, Cui KM, Itoh T (2002) Toward understanding the different function of two types of parenchyma cells in bamboo culms. Plant Cell Physiol 2:186-195.

Komuraiah A, Shyam Kumar N, Durga Prasad B (2014) Chemical composition of natural fibers and its influence on their mechanical properties. Mech Compos Mater 3:509-528.

Larsen KL, Barsberg S (2010) Theoretical and Raman spectroscopic studies of phenolic lignin model monomers. J Phys Chem 114:8009-8021.

Lin JX, He XQ, Hu YX, Kuang TY, Ceulemans R (2002) Lignification and lignin heterogeneity for various age classes of bamboo (*Phyllostachys pubescens*) stems. Physiol Plant 2:296-302.

Lybeer B, Koch G (2005a) Lignin distribution in the tropical bamboo species *Gigantochloalevis*. IAWA J 4:445-456.

Lybeer B, Koch G (2005b) A topochemical and semiquantitative study of the lignifications during ageing of bamboo culms (*Phyllostachys viridiglaucescens*). IAWA J 1:99-109.

Lybeer B, Van Acker J, Goetghebeur P (2006) Variability in fibre and parenchyma cell walls of temperate and tropical bamboo culms of different ages. Wood Sci Technol 40:477-492.

Ma JF, Yang GH, Mao JZ, Xu F (2011) Characterization of anatomy, ultrastructure and lignin microdistribution in Forsythia suspense. Ind Crops Prod 33:358-363.

Merk V, Chanana M, Gierlinger N, Hirt AM, Burgert I (2014) Hybrid wood materials with magnetic anisotropy dictated by the hierarchical cell structure. ASC Appl Mater Interfaces 6:9760-9767.

Mustafa MT, Wahab R, Sudin M, Sulaiman O, Kamal NAM, Khalid L (2011) Anatomical and microstructures features of tropical bamboo *Gigantochloa brang*, *G. levis, G. scotechinii* and *G. wrayi*. Int J Forest Soil and Erosion 1:25-35.

Parameswaran N, Liese W (1976) On the fine structure of bamboo fibres. Wood Sci Technol 10:231-264.

Ram MS, Dowell FE, Seitz LM (2003) FT-Raman spectra of unsoaked and NaOH-soaked wheat kernels, bran, and ferulic acid. Cereal Chem 80:188-192.

Richter S, Müssig J, Gierlinger N (2011) Functional plant cell wall design revealed by the Raman imaging approach. Planta 233:763-772.

Röder T, Koch G, Sixta H (2004) Application of confocal Raman spectroscopy for the topochemical distribution of lignin and cellulose in plant cell walls of beech wood (*Fagus sylvatica* L.) compared to UV microspectrophotometry. Holzforschung 58:480-482.

Saariaho AM, Jääskeläinen AS, Nuopponen M, Vuorinen T (2003) Ultraviolet resonance raman spectroscopy in lignin

analysis: Determination of characteristic vibrations of p-hydroxyphenyl, guaiacyl, and syringyl lignin structures. Appl Spectrosc 1:58-66.

Saka S, Thomas RJ (1982) A study of lignification in loblolly pine tracheids by the SEM-EDXA technique. Wood Sci Technol 16:167-179.

Sun L, Blake AS, Singh S (2010) Understanding tissue specific compositions of bioenergy feedstocks through hyperspectral Raman imaging. Biotechnol Bioeng 2:286-295.

Sun L, Varanasi P, Yang F, Loqué D, Simmons BA, Singh S (2012) Rapid determination of syringyl: Guaiacyl ratios using FT-Raman spectroscopy. Biotechnol Bioeng 109: 647-656.

Wang XQ, Keplinger T, Gierlinger N, Burgert I (2014) Plant material features responsible for bamboo's excellent mechanical performance: A comparison of tensile properties of bamboo and spruce at the tissue fibre and cell wall levels. Ann Bot 8:2-9.

Wang XQ, Ren HQ, Zhang B, Fei BH, Burgert I (2012) Cell wall structure and formation of maturing fibres of mosobamboo (*Phyllostachys pubescens*) increase buckling resistance. J R Soc Interface 9:988-996.

Wi SG, Lee KH, Bae HJ, Bae HJ, Park BD, Singh AP (2014) Variability in the distribution of middle lamella lignin in secondary vascular tissues of kenaf stems. IAWA J 1:61-68.

Zhang SY, Wang CG, Fei BH, Yu Y, Cheng HT, Tian GL (2013) Mechanical function of lignin and hemicelluloses in wood cell wall revealed with microtension of single wood fiber. Bioresoures 2:2376-2385.